Correlation of Marine 14 C Ages from the Nordic Seas with the GISP2 Isotope Record: Implications for 14 C Calibration Beyond 25 ka BP

Antje Voelker, Michael Sarnthein, Pieter Grootes, Helmut Erlenkeuser, Carlo Laj, Alain Mazaud, Marie-Josée Nadeau, Markus Schleicher

CORRELATION OF MARINE ^{14}C AGES FROM THE NORDIC SEAS WITH THE GISP2 ISOTOPE RECORD: IMPLICATIONS FOR ^{14}C CALIBRATION BEYOND 25 ka BP

ANTJE H. L. VOELKER,[1] MICHAEL SARNTHEIN,[1] PIETER M. GROOTES[2]
HELMUT ERLENKEUSER,[2] CARLO LAJ,[3] ALAIN MAZAUD,[3] MARIE-JOSÉE NADEAU[2]
and MARKUS SCHLEICHER[2]

ABSTRACT. We present two new high-resolution sediment records from the southwestern Iceland and Norwegian Seas that were dated by numerous ^{14}C ages up to 54 ^{14}C ka BP. Based on various lines of evidence, the local ^{14}C reservoir effect was restricted to 400–1600 yr. The planktic stable isotope records reveal several meltwater spikes that were sampled with an aver-age time resolution of 50 yr in PS2644 and 130 yr in core 23071 during isotope stage 3. Most of the $\delta^{18}O$ spikes correlate peak-by-peak to the stadials and cold rebounds of the Dansgaard-Oeschger cycles in the annual-layer counted GISP2 ice core, with the major spikes reflecting the Heinrich events 1–6. This correlation indicates large fluctuations in the calibration of ^{14}C ages between 20 and 54 ^{14}C ka BP. Generally the results confirm the ^{14}C age shifts as predicted by the geomagnetic model of Laj, Mazaud and Duplessy (1996). However, the amplitude and speed of the abrupt decrease and subsequent major increase of our ^{14}C shifts after 45 ^{14}C ka BP clearly exceed the geomagnetic prediction near 40–43 and 32–34 calendar (cal) ka BP. At these times, the geomagnetic field intensity minima linked to the Laschamp and the Mono Lake excursions and confirmed by a local geomagnetic record, probably led to a sudden increase in cosmogenic ^{14}C and [10]Be production, giving rise to excess ^{14}C in the atmosphere of up to 1200‰.

INTRODUCTION

Laj, Mazaud and Duplessy (1996) presented a geomagnetic field-intensity record, mainly based on three magnetic records from deep-sea sediments in the Azores Basin (Lehman *et al.* 1996), and cal-culated from this evidence a global ^{14}C production curve for the last 80 cal ka BP. To examine the differential contributions of both the Earth's magnetic field and the ventilation of the deep ocean to variations in the atmospheric ^{14}C budget, they employed a simple four-box global ocean model to convert the geomagnetic ^{14}C production curve into a record of bulk past changes in the atmospheric ^{14}C/^{12}C ratio (referred to as $\Delta^{14}C$). They found that 80% of the $\Delta^{14}C$ variations (and thus the major shifts between ^{14}C and calendar ages) over the last 50 ^{14}C ka BP can be explained by changes in the geomagnetic field and only 20% by changes in ocean ventilation. For the last 20 ^{14}C ka BP, their pro-posed ^{14}C age shifts are well confirmed by dendro- and lake-varve chronology (Stuiver and Reimer 1993; Kromer and Becker 1993; Goslar *et al.* 1995) and various spot calibrations (Bard *et al.* 1990; Bard *et al.* 1993; Edwards *et al.* 1993). Hardly any proof hitherto existed for the calibration of ^{14}C ages >20 ^{14}C ka BP (Chappell and Veeh 1978; Vogel 1983; Bard *et al.* 1993, 1998).

The GISP2 ice core from the Greenland summit may bridge this gap by providing a unique annual-layer counted time scale for the last 50 ka BP (Meese *et al.* 1994). The paleoclimatic $\delta^{18}O$ signals used have a resolution of 1 m, equal to a time resolution of 40–60 yr for the interval 12–50 cal ka BP (Grootes and Stuiver 1997; *cf.* Fig. 2 below). However, the annual-layer dated $\delta^{18}O$ record in the GISP2 ice core cannot be used directly to calibrate ^{14}C ages because of the difficulty of dating atmo-spheric CO_2 trapped in the ice core (Wilson 1995; Wahlen, personal communication 1997). We thus employ a different strategy to convert the annual-layer time scale. First, we correlate the $\delta^{18}O$ tem-perature record of GISP2 step-by-step to two high-resolution sediment records of climatic change from the nearby Nordic Seas. In a second step, the marine ^{14}C ages of the various correlated climatic

[1]Geologisch-Paläontologisches Institut, Universität Kiel, Olshausenstrasse 40, D-24118 Kiel, Germany
[2]Leibniz Labor für Altersbestimmung und Isotopenforschung, Universität Kiel, Olshausenstrasse 40, D-24118 Kiel, Germany
[3]Centre des Faibles Radioactivités, Laboratoire mixte CEA-CNRS, Avenue de la Terrasse, F-91198 Gif-sur-Yvette, France

events are linked to the annual-layer counted chronology of the GISP2 ice core. This provides the framework for the ^{14}C age anomalies from the calendar time scale over the last 50 ka BP.

METHODS

We studied two deep-sea cores from the western and eastern Nordic Seas, which have sedimentation rates of 8–20 cm ka^{-1} during stage 3 (Fig. 1). We focused especially on the "watch dog" position of site PS2644 (67°52.02′N, 21°45.92′W; 777 m water depth; 9.18 m core recovery) in the West Iceland Basin to monitor changes in the surface and intermediate water currents through the Denmark Strait (Hopkins 1991) (Fig. 1). Today, the hydrographic conditions near site PS2644 show a high interseasonal and interannual (and spatial) variability, such as with the "Great Salinity Anomaly" during the 1960s (Malmberg and Stefansson 1972; Malmberg 1984; Malmberg and Kristmannsson 1992). In particular, the site occupies a position right in between 1) the warm, saline Atlantic water of the North Icelandic Irminger Current (NIIC) to the south; 2) the cold, freshwater-enriched East Greenland Current (EGC), which carries plenty of drift ice and icebergs, to the north and west; and 3) the East Iceland Current (EIC), an easterly branch of the EGC, to the northeast (Stefansson 1962; Swift and Aagaard 1981; Hopkins 1991) (Fig. 1). Sea ice covers site PS2644 during winter and spring, and occasionally also during summer (Vinje 1977; Malmberg 1984).

During glacial times, the site of PS2644 was reached by icebergs and meltwater originating from both Iceland and East Greenland (Voelker *et al.* 1997). PS2644 was then located at the entrance of a shallower Denmark Strait, narrowed down by the adjacent continental ice shields. The Icelandic glaciers extended about 130 km onto the western Icelandic shelf during the Last Glacial Maximum (LGM; *ca.* 20 cal ka BP) (Olafsdóttir 1975; Vogt, Johnson and Kristjansson 1980), whereas off the Kangerdlugssuaq Fjord on the western side of the Denmark Strait the ice margin reached >100 km onto the shelf (Larsen 1983 and references therein; Andrews *et al.* 1996).
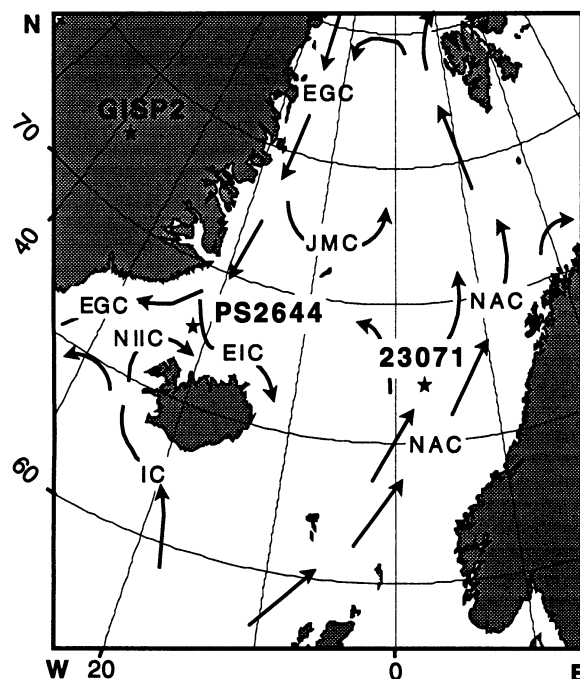
Fig. 1. Location (★) of sediment cores PS2644 and GIK23071 in the Icelandic and Norwegian Seas and the GISP2 ice core on Greenland. ↗ = present axes of the major currents in the Nordic Seas (EGC: East Greenland; EIC: East Iceland; IC: Irminger; JMC: Jan Mayen; NAC: Norwegian Atlantic; NIIC: North Iceland Irminger).

Core 23071 (67°05.09′N, 2°54.48′E, 1308 m water depth; 7.23 m core recovery) was retrieved on the Voering Plateau in the Norwegian Sea (Fig. 1). The site is located below the warm, saline Norwegian Atlantic Current, which provides ice-free conditions in the Norwegian Sea throughout the year (Swift and Aagaard 1981; Hopkins 1991). During glacial periods this site was reached by icebergs and meltwater originating from the Fennoscandian ice sheets (*e.g.*, Fronval *et al.* 1995).

The δ^{18}O and δ^{13}C records are based on a 1-cm sampling resolution, equal to a mean time resolution of 50 yr for PS2644 and 130 yr for 23071 in marine oxygen isotope stage 3 (Fig. 2). The stable isotopes were measured on samples of 30 specimens of the polar planktic foraminifer *Neogloboquadrina (N.) pachyderma* (sinistral) (125–250 μm). The foraminifera specimens were neither treated with alcohol nor cracked and cleaned in an ultrasonic bath, because we believe the contamination by coccolithophorids to be small based on the low carbonate content of the sediments and SEM studies. In the record of core 23071, we include previously published data from Sarnthein *et al.* (1995). The stable isotope data were measured in the MAT-251 mass spectrometer of the Leibniz Labor of Kiel University, which runs with the automated Carbo-Kiel preparation line and has an analytical reproducibility of ±0.07‰ for δ^{18}O and ±0.04 ‰ for δ^{13}C (Sarnthein *et al.* 1995). The isotope values are calibrated to the Peedee Belemnite (PDB) scale *via* National Bureau of Standards standard NBS 19.

To roughly interpret the planktic δ^{18}O curve in terms of a paleosalinity record, we counted in the >150 μm fraction of core PS2644 1) the percentage of *N. pachyderma* (sinistral) as a proxy for paleo-sea-surface temperatures (Bond *et al.* 1993; Cortijo 1995), and 2) the abundance of lithic fragments as proxy for ice-rafted debris to identify iceberg incursions (Ruddiman 1977; Bond and Lotti 1995) (Fig. 3). Furthermore, we used rhyolithic shards and basaltic ash particles (not depicted in this paper) to identify 1) iceberg meltwater originating from Iceland and 2) North Atlantic Ash Zones 1 and 2. These are employed as major stratigraphic markers and can be clearly distinguished in the Greenland ice core records (Grönvold *et al.* 1995; Zielinski *et al.* 1996).

Our results on ^{14}C fluctuations were linked to the geomagnetic model of Laj, Mazaud and Duplessy (1996) by measuring the natural remanent magnetization (NRM) in the continuous high-resolution u-channel profile of PS2644 (method of Weeks *et al.* 1993). We normalized NRM with anhysteretic remanent magnetization (ARM), isothermal remanent magnetization (IRM), and susceptibility (Fig. 4). Inclination and declination records were also obtained.

The planktic AMS ^{14}C ages of both cores (Appendix: Table 1A,B; Fig. 2) were measured on monospecific samples of the planktic foraminifer *N. pachyderma* (sin.) (150–250 μm; 800–2300 specimens). We also obtained a few benthic AMS ^{14}C ages from either mixed or monospecific samples of the epibenthic foraminifera species *Cibicides lobatulus* (Walker & Jacob) and *Cibicidoides pachyderma* (Rzehak) from PS2644 (100–240 specimens; Table 2). The AMS samples were strictly selected on the basis of abundance maxima of the foraminifera species to minimize bioturbation effects. Most samples were washed with distilled water in an ultrasonic bath before further treatment. A set of the oldest samples with KIA numbers ≥3506 were washed with peroxide and then attached to the carbonate system while still wet (Schleicher *et al.* 1998) to obtain the lowest background correction. The three samples of PS2644 measured at the Gif-sur-Yvette AMS facility (Table 1A) were treated according to that laboratory's procedures (Arnold *et al.* 1989). Most samples were measured in the Kiel Leibniz-Labor AMS facility (3 MV HVEE Tandetron 4130 AMS) (Nadeau *et al.* 1997) with a background age of 46 ka BP for foraminiferal samples prior to July 1997 (Schleicher *et al.* 1998) and background ages of 51–57 ka BP with the "wet" peroxide treatment (Table 1A, B). A number of dates of core 23071 were measured in Gif-sur-Yvette (Sarnthein *et al.* 1995) and Aarhus (Samtleben *et al.* 1995) and are included in this study. The >130 datings of core PS2644 lead to an approximate sample spacing of 3 dates per 1000 yr.
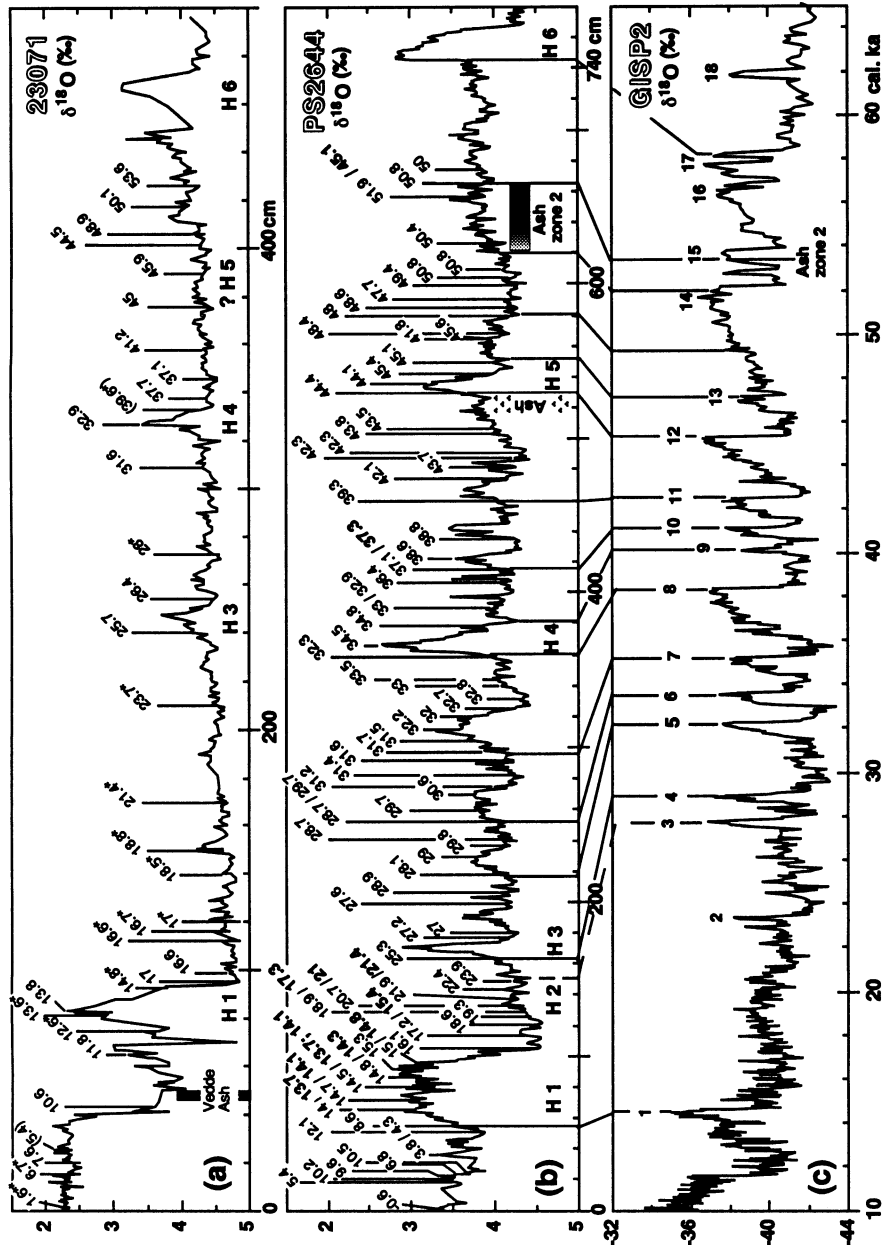
Fig. 2. Planktic $\delta^{18}O$ stratigraphy based on *N. pachyderma* (sinistral) in cores (a) GIK23071 and (b) PS 2644 *vs.* depth. Oblique numbers show AMS ^{14}C dates in ka BP (Table 1A+B), measured on planktic *N. pachyderma* (sin.) (plain) and benthic foraminifera (bold) (Table 2), corrected for an oceanic reservoir effect of 400 yr. For PS2644 only weighted average ages are shown below 4.88 m composite depth. * = ages measured in Gif-sur-Yvette by M. Arnold. H1–H6 indicate Heinrich events 1 to 6. (c) $\delta^{18}O$ record of annual-layer dated GISP2 ice core (in ka BP; Grootes and Stuiver 1997), used for chronostratigraphic comparison and the calibration of ^{14}C ages. Numbers refer to "Dansgaard–Oeschger" interstadials (Johnsen *et al.* 1992). Vertical lines show correlation of Dansgaard–Oeschger events in GISP2 with pertinent events in the $\delta^{18}O$ record of PS2644 (dashed line is tentative correlation).
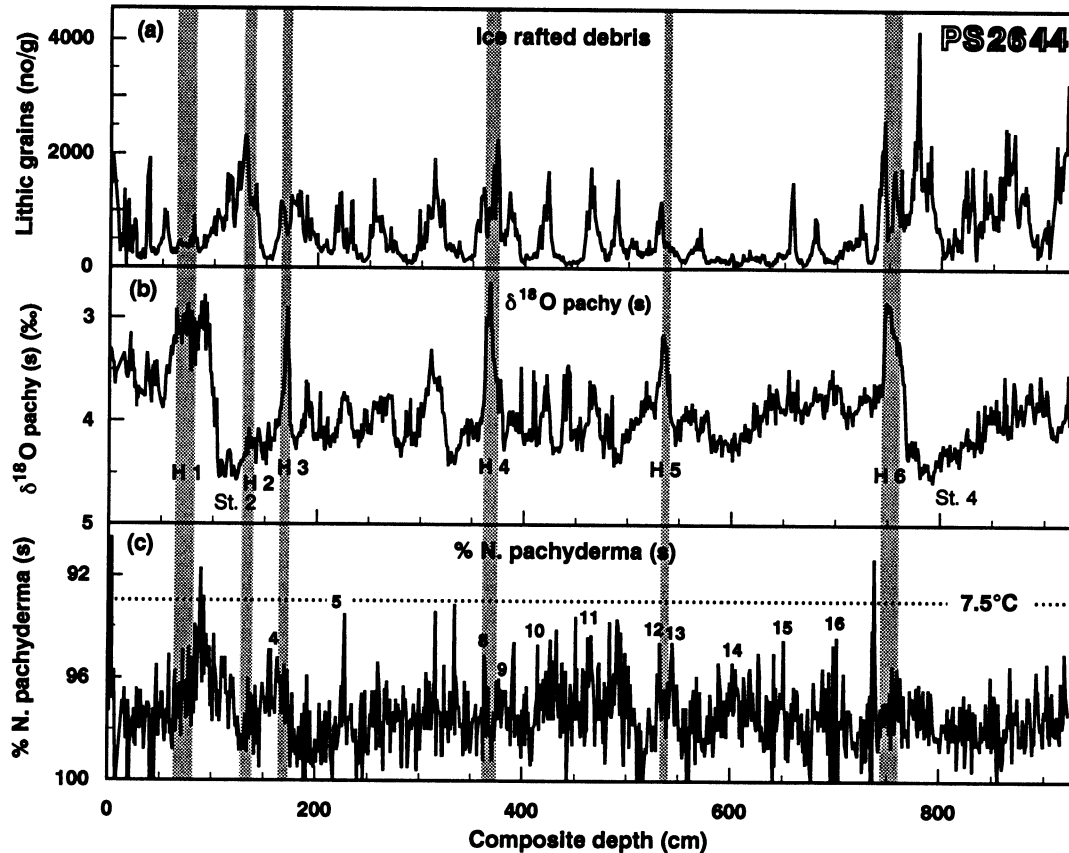
Fig. 3. Lithic grain concentration in (a) fraction >150 μm, (b) planktic δ¹⁸O record, and (c; reversed) percentages of planktic foraminifera *N. pachyderma* (sinistral) in the fraction >150 μm of core PS2644 *vs.* composite core depth. The lithic grain concentration serves as a proxy for the ice-rafted debris, supplied by melting icebergs. Peak abundances correlate with meltwater spikes *(i.e.,* minima) in the planktic δ¹⁸O record and with glacial stages 2 and 4 (St. 2, 4). H1–H6 indicate Heinrich meltwater events 1–6. Low percentages of *N. pachyderma* (sin.), a proxy for sea-surface temperatures, mainly correlate with heavier δ¹⁸O values following a δ¹⁸O depletion. They indicate the advection of warm Atlantic water into the Iceland Sea contemporary with warming episodes on Greenland (numbers mark ice-core interstadials; Johnsen *et al.* 1992). ····· = the percentage for 7.5°C surface water temperature (Cortijo 1995).

In summary, the stratigraphy in both cores is based on Ash Zone 2 in core PS2644, the AMS ^{14}C ages and on tuning the stable isotope records to the GISP2 ice core.

PALEO-RESERVOIR EFFECT

We measured the benthic AMS ^{14}C ages to obtain ventilation ages of the glacial intermediate/deep-water masses identified in the benthic stable isotopes of PS2644 (Voelker, Sarnthein and Erlen-keuser 1996). We expected benthic ages that were higher than the planktic ages according to the generally observed gradual aging of deepwater (Andree *et al.* 1986; Broecker *et al.* 1988). However, as shown in Table 2, most benthic ages are younger than the planktic ages measured at the same core depth. The age differences reach up to 1600 yr (we excluded benthic ages at 1.63 m and 2.52 m based on the small sample size of <0.5 mg C, as well as an extreme outlier at 6.57 m). The benthic-planktic age anomalies cannot be explained by differential bioturbation, since bioturbational mixing
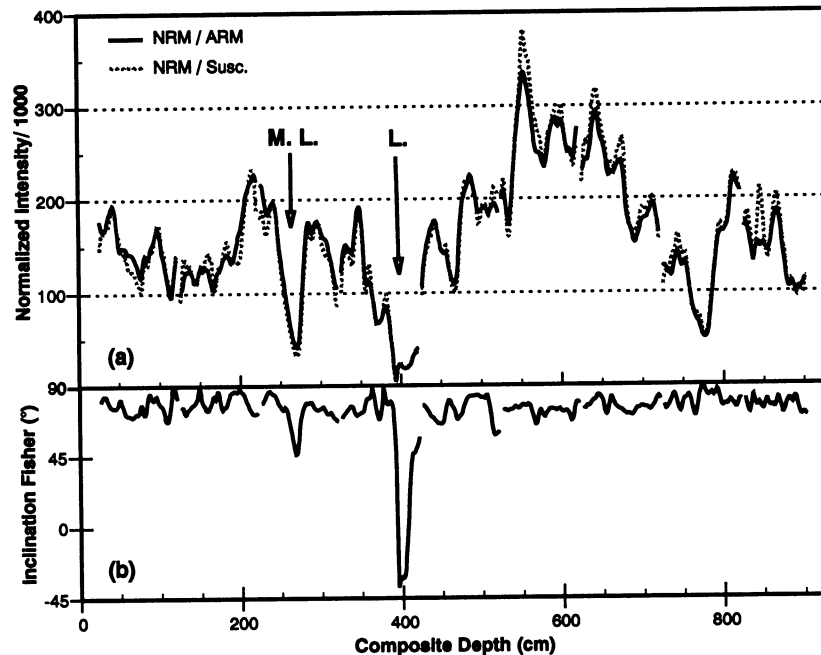
Fig. 4. Two normalized magnetic field intensity records (a) and the inclination record (b) *vs.* depth
obtained in core PS2644. Normalizing parameters for the natural remanent magnetization (NRM) are
the anhysteretic remanent magnetization (ARM) (black curve) and the susceptibility (gray curve).
M.L. = Mono Lake Excursion; L. = Laschamp Excursion.

is almost negligible in regions where the nutrient flux is extremely low (Trauth, Sarnthein and
Arnold 1997). Most planktic ^{14}C ages of Heinrich events in 23071 were younger than the planktic
ages and similar to the benthic ages measured on the same Heinrich events in core PS2644. In the
Southern Ocean, several areas are covered by seasonal ice leading to an increase of reservoir ages
of the surface water to 1300 yr (Gordon and Harkness 1992; Stuiver and Braziunas 1993; Berkman
and Forman 1996) and up to 5500 yr (Domack *et al.* 1989). Per analogy, we infer a paleo-reservoir
effect for the planktic ^{14}C ages off Iceland, which by far exceeds the conventional number of 400 yr.
This paleo-reservoir effect does not occur in the probably largely ice-free Norwegian Sea (Sarnthein
et al. 1995) where glacial deepwater has formed (Weinelt *et al.* 1996; Seidov *et al.* 1996) and con-
sequently, the water column has been thoroughly mixed.This young glacial deepwater also passed
the Denmark Strait as recorded in the "young" benthic AMS ^{14}C ages of PS2644.

The high and variable paleo-reservoir effect northwest of Iceland was probably caused by changes
in the habitat of the planktic foraminifer *N. pachyderma* (sin.). It may have calcified its tests in local
"oldish" subsurface and/or upper intermediate waters that were less ventilated below sea-ice cover
and/or meltwater lids. These assumptions fit recent observations in the modern Arctic ocean (Bauch,
Carstens and Wefer 1997) and in the Greenland Sea (Simstich *et al.*, ms.). Below the modern fresh-
water-enriched and partly ice-covered West Greenland and Labrador Currents, Wu and Hillaire-
Marcel (1994) also obtained negative benthic-planktic age differences of −350 to −2110 yr in late
Holocene sediment samples from the continental margin off southern Greenland and from the
Labrador Sea.

TABLE 2. Calculation of Benthic–Planktic Age Differences in Core PS2644

Depth (m)	Benthic species and size fraction*	Benthic AMS ¹⁴C age ±1σ (yr)	Planktic AMS ¹⁴C age ±1σ (yr)	Δ Benthic–Planktic ±1σ (yr)
0.65	*Cibicides lobatulus + Cibicidoides pachyderma* > 250 μm	13,650 ± 90	13,970 ± 60	−320 ± 110
0.71	*Cibicides lobatulus + Cibicidoides pachyderma* > 150 μm	14,050 ± 80	14,680 ± 210	−630 ± 220
0.80	*Cibicides lobatulus + Cibicidoides pachyderma* > 315 μm	14,090 ± 90	14,490 ± 80	−400 ± 120
0.80	*Cibicidoides pachyderma* > 400 μm	13,730 ± 90	14,490 ± 80	−760 ± 120
0.86	*Cibicides lobatulus + Cibicidoides pachyderma* > 150 μm	14,320 +90/−80	14,810 ± 240	−490 +250/−260
0.95	*Cibicides lobatulus + Cibicidoides pachyderma* > 150 μm	14,750 ± 80	14,980 ± 90	−230 ± 120
1.13 (1.13–1.14)	*Cibicides lobatulus + Cibicidoides pachyderma* > 250 μm	15,790 ± 120	17,230 ± 90	−1440 ± 150
1.29	*Cibicides lobatulus* > 250 μm	17,340 ± 160	18,900 ± 90	−1560 ± 180
1.33	*Cibicides lobatulus* > 250 μm	21,030 ± 200	20,700 ± 160	330 ± 260
1.37	*Cibicides lobatulus* > 150 μm	21,390 +200/−190	21,940 ± 180	−550 +260/−270
1.63 (1.62–1.64)	*Cibicides lobatulus + Cibicidoides pachyderma* > 150 μm	23,380 +220/−210	25,300 +300/−290	−1920 +370/−360†
2.52 (2.50–2.54)	*Cibicides lobatulus* > 150 μm	25,200 +420/−400	28,650 +420/−400 29,740 +270/−260	−3450 ± 580† −4540 +480/−490†
4.14 (4.13–4.15)	*Cibicides lobatulus* > 150 μm	37,340 +1190/−1040	37,050 +1400/−1190	290 +1680/−1740
6.57 (6.56 –6.58)	*Cibicides lobatulus* > 250 μm	45,110 +1360/−1170	51,870 +1670/−1380	−6760 +2040/−1940†

*The bulk of benthic foraminifera were picked from the >315 μm fraction. Smaller size fractions were used, when samples from the larger fractions were too small.
† Problematic age anomaly ignored (see text).

To test the assumption of increased and highly variable paleo-reservoir ages, the regional distribution of ¹⁴C ages at the base of Heinrich Event 4 was mapped using the age records of 22 deep-sea cores from the North Atlantic (Sarnthein *et al.*, unpublished data). Along the main track of meltwater input during Heinrich Event 4, as reconstructed from planktic δ¹⁸O values (Cortijo *et al.* 1997), planktic ¹⁴C ages vary between 35 and 36.5 ka BP, whereas at peripheral sites the ages decrease to

33.5–34 ka BP. The resulting age differences exceed 1500 yr. Likewise, a model on the influence of Heinrich-type meltwater events on the oceanic ^{14}C budget (Stocker and Wright 1998) shows reservoir ages that strongly vary, independently for surface and deepwater in the Atlantic at 39°N, near the southern edge of the major meltwater track (Cortijo *et al.* 1997). Moreover, Bard *et al.* (1994) and Haflidason, Seirup, and Kristensen (1996) measured an increased paleo-reservoir effect of >800 yr for the North Atlantic at the Vedde Ash during the Younger Dryas.

For calibrating the marine ^{14}C time scale to the GISP2 calendar time scale, however, we used the ^{14}C ages of PS2644 with a simple constant ocean reservoir age of 400 yr because of an insufficient number of benthic ages. Without correction, any increase in the reservoir effect would result in an (apparent) increase of the ^{14}C age and hence, in a decrease of the (apparent) ^{14}C age shift.

CORRELATION WITH GISP2

Any correlation between the marine climate record of core PS2644 and the GISP2 isotope-temperature record requires a basic understanding of the planktic stable-isotope signals. In the marine record, most δ^{18}O minima run parallel to 1) δ^{13}C minima, indicating reduced ventilation of the surface ocean (Sarnthein *et al.* 1995; Fig. 5), 2) high values of ice-rafted debris (Fig. 3), and 3) high percentages of *N. pachyderma* (sin.), indicative of cold surface water temperatures (Fig. 3). This evidence links most δ^{18}O minima to meltwater events, not to increased sea-surface temperatures. An exception is found at the δ^{18}O minimum prior to Heinrich event 1, which is clearly identified as a warm event by lower percentages (down to 92%) of *N. pachyderma* (sin.). Based on the equation of Cortijo (1995), a percentage of 93% already corresponds to a sea-surface temperature of 7.5°C, whereas higher abundances cover the whole temperature range from 0–7.5°C. At site PS2644, these lower percentages indicate an occasional advection of warm Atlantic water across the Denmark Strait, a paleo-Irminger Current. They match "heavier" δ^{18}O and δ^{13}C values and often follow a meltwater event (Fig. 3), similar to the observations of Rasmussen *et al.* (1996a,b) in core ENAM 93–21 at the margin of the Faeroe-Shetland Channel.

The most prominent δ^{18}O minima in cores PS2644 and 23071 correspond to the Heinrich meltwater events (H1–H6) in the North Atlantic, that Bond *et al.* (1993) related to the cold stadials preceeding the Dansgaard-Oeschger interstadials 1, 2, 4, 8, 12, and 17 in the Greenland ice cores (Fig. 2). Based on the same interpretative rules, we can relate the numerous minor δ^{18}O depletions to the less pronounced cold phases in the GISP2 isotope-temperature record, approximately matching the spike amplitudes. The onset of the planktic δ^{18}O meltwater signal is directly linked to the abrupt cooling episodes ending the interstadials or defining abrupt steps in their decline. By contrast, every final disappearance of meltwater matches phases of abrupt temperature increase on Greenland (Fig. 5; note that the planktic δ^{18}O record is plotted in normal order to demonstrate the correlation of minima and maxima in the δ^{18}O records measured in ice and marine sediments). The meltwater disappearance is indicated by an abrupt increase in the planktic δ^{13}C values, *i.e.*, the appearance of well ventilated surface water, that is accompanied by the advection of Atlantic water (lower percentage of *N. pachyderma* (sin.)) and indicates a return to the interstadial mode of the thermohaline circulation (Rasmussen *et al.* 1996a,b). Furthermore, the onsets of Dansgaard-Oeschger events 1–13, 16, 18, and 19 are marked by a pronounced increase in the abundance of *Cibicides* sp. (Voelker, unpublished data), benthic species that indicate strong bottom currents (Mackensen, Sejrup and Jansen 1985) and thus, the overflow of glacial deep water. The warm phases in the sediment record are also associated with high magnetic susceptibility values (Niessen *et al.* 1996) which helped to solve minor correlation problems near Dansgaard-Oeschger events 9–11. Here the signal frequency is higher in core PS2644 than in the GISP2 isotope-temperature record, a difference yet unexplained.
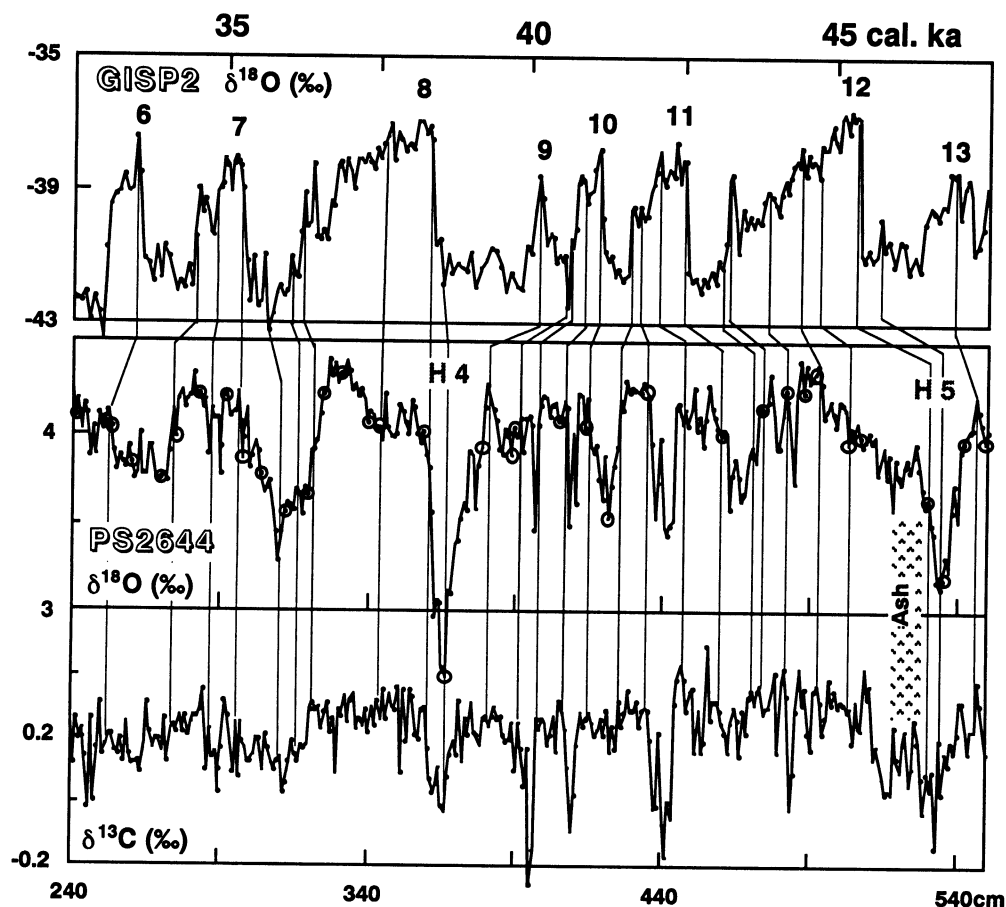
Fig. 5. Close-up of the correlation between Dansgaard-Oeschger cycles 6–13 in the GISP2 δ^{18}O record (Grootes and Stuiver 1997) and the planktic δ^{18}O and δ^{13}C records in core PS2644. O = position of ^{14}C ages. H4 and H5 refer to Heinrich events 4 and 5.

The low time resolution of the climatic oscillations in PS2644 between H3 and H1, their fairly low amplitudes, and a potential hiatus subsequent to Heinrich event 2 hamper a precise age correlation between *ca.* 17 to 26 cal ka BP.

The cumulative error in the GISP2 time scale (Meese *et al.* 1994) is ignored. For the interval we study, this uncertainty in the number of counted layers is small as compared to other age uncertainties considered here.

CALIBRATION OF ^{14}C AGES

Our correlation reveals differences between the marine ^{14}C and the GISP2 calendar ages as shown in Figure 6 *(Color Plate 1, following p. 416)*. The reconstructed ^{14}C age shifts (in Libby years) generally confirm the predicted calibration curve of Laj, Mazaud and Duplessy (1996), based on their geomagnetic model (in ^{14}C years based on $T_{1/2}$ = 5730 yr; x-axis is the inclined $T_{1/2}$ correction line). In particular, the expected abrupt increase in the age shift between 45 and 37 ka BP is generally verified. Also, from 25 to 10 ka BP, our shifts of 3700 to 1300 yr nicely fit the model within the predicted error range and are in accordance with the other published data sets on ^{14}C age calibration.

However, we observe a new minimum ^{14}C age shift of 150–1000 yr near 44–45 ka BP and two prominent intervals near 33–34 and 28.5 ka BP where our reconstructed age shifts rise to 7600 yr and 4800 yr, respectively, thus exceeding the predictions by a factor of 2.7 and 1.5 (Fig. 6). Along with the 7600 yr shift, the ^{14}C ages "jump" forward by 3500 ^{14}C yr within 0.15 m core depth in core PS2644 (Fig. 2; Table 1A). Our abrupt and extreme increases in ^{14}C activity exactly coincide with two marked lows of geomagnetic field intensity, measured in core PS2644 at 3.86–4.16 m and 2.60–2.75 m composite depth (Fig. 4). The intensity minima are attributed to the Laschamp and the Mono Lake excursions (Bonhommet and Babkine 1967; Denham and Cox 1971), as revealed by the inclination changes of >90° and >20°, previously ^{14}C-dated at *ca.* 33 ka BP (Vlag *et al.* 1996) and 28 ka BP (Liddicoat 1992), respectively. The extremely reduced age shifts near 44–45 ka BP actually form negative age shifts, with respect to the physical half-life of 5730 yr. They may result from the preceeding long-term increase in geomagnetic field intensity, ending near 5.50 m in core PS2644, a level which was dated at 45 ka BP (Fig. 4 and 2).

The Azores geomagnetic record, upon which the model of Laj, Mazaud and Duplessy (1996) is based, was derived from sediments with relatively low sedimentation rates. Thus the mechanisms of sedimentary magnetization acquisition possibly smoothed the effects of the fast-changing geomagnetic field, resulting in broader, less pronounced minima and consequently, in lower values of calculated ^{14}C production. Analyses of paleointensity records from ODP site 983 (Channell, Hodell and Lehman 1997), offering a time resolution similar to PS2644, confirm the large and rapid magnetic variability found in PS2644.

Our extreme ^{14}C age shifts at the Laschamp and Mono Lake events appear trustworthy because they are based on multiple planktic and benthic datings in cores PS2644 and 23071. The shifts are further supported by various spot calibrations based on concurrent ^{14}C and U/Th dates (Chappell and Veeh 1978; Vogel 1983; Schramm, Stein and Goldstein 1996, 1997; Vogel and Kronfeld 1997; Bard *et al.* 1998; Geyh and Schlüchter 1998). Our reconstructed age shifts are in line with findings of McIntyre and Molfino (1996), who obtained similar age shifts from a record in the equatorial Atlantic by using the calibration of Stuiver and Reimer (1993) and Bard *et al.* (1993). On the other hand, Kitagawa and van der Plicht (1998) calibrated ^{14}C ages of terrestrial organic matter with varve ages in Lake Suigetsu, Japan, and observe a ^{14}C age shift of 4700 yr at 25.5–26.5 ka BP, which may resemble our Mono Lake event, but is about 2500 ^{14}C yr younger.

Our maximum age shifts correspond, if calculated with the physical ^{14}C half-life of 5730 yr, to peak atmospheric Δ^{14}C values of *ca.* +1200‰ during the Laschamp event and +670‰ during the Mono Lake excursion (Fig. 6). These high cosmogenic ^{14}C concentrations are confirmed by the coeval cosmogenic [10]Be peaks observed in ice cores (Raisbeck *et al.* 1987; Beer *et al.* 1992; Yiou *et al.* 1997) and marine sediment records (McHargue, Damon and Donahue 1995; Castagnoli *et al.* 1995; Robinson *et al.* 1995; Frank *et al.* 1997) and by high [36]Cl/[35]Cl ratios in fossil packrat urine (Plummer *et al.* 1997).

CONCLUSION

Detailed correlation of our ^{14}C-dated sediment cores PS2644 and 23071 with the GIPS2 ice core, dated by layer counting, provides a considerable number of ^{14}C calibration points revealing large fluctuations in ^{14}C concentration in planktic foraminifera. In general, our data confirm the geomagnetic model of atmospheric Δ^{14}C changes as presented by Laj, Mazaud and Duplessy (1996). However, our record of ^{14}C age shifts over the last 52 ^{14}C ka BP does not provide a simple key for converting marine ^{14}C ages beyond 20 ^{14}C ka BP into calendar ages due to still insufficient data and,

probably, local and variable reservoir age effects. Such calendar ages are essential to calculate sedimentation rates and material balances or to elucidate the timing and driving mechanisms of rapid climatic changes.

Based on our data, jumps in the ${}^{14}C$ shifts can amount to >7500 yr and >4500 yr at the Laschamp and Mono Lake geomagnetic events, respectively, and probably account for many age reversals observed in marine and terrestrial records, especially during 33–35 ka BP. The observed fast changes in atmospheric $\Delta^{14}C$ need further detailed calibrations in sediments from land, such as the record provided by Kitagawa and van der Plicht (1998), and from the ocean to establish the details of the various jumps and plateaus of the ${}^{14}C$ time scale. New high-resolution geomagnetic records (such as that of Fig. 4) and a more sophisticated treatment of the global oceanic circulation will provide a better understanding of the primary cosmogenic ${}^{14}C$ production rates that may have reached >220% of the modern rate, and of the potential impact of variations in the ocean circulation and in the ocean-atmosphere exchange on past changes in the atmospheric ${}^{14}C$ budget.

ACKNOWLEDGMENTS

REFERENCES

Andree, M., Oeschger, H., Broecker, W. S., Beavan, N., Klas, M., Mix, A., Bonani, G., Hofmann. H. J., Suter, M., Woelfli, W. and Peng, T.-H. 1986 Limits on the ventilation rate for the deep ocean over the last 12,000 years. *Climate Dynamics* 1: 53–62.

Andrews, J. T., Jennings, A. E., Cooper, T., Williams, K. M. and Mienert, J. 1996 Late Quaternary sedimentation along a fjord to shelf (trough) transect, East Greenland (*c.* 68°N). *In* Andrews, J. T., Austin, W. E. N., Bergsten, H. and Jennings, A. E., eds., *Late Quaternary Palaeoceanography of the North Atlantic Margins*. Geological Society Special Publication no. 111, London: 153–166.

Arnold, M., Bard, E., Maurice, P., Valladas, H. and Duplessy, J.-C. 1989 ${}^{14}C$ Dating with the Gif-sur-Yvette Tandetron accelerator: Status report and study of isotopic fractionation in the sputter ion source. *In* Long, A., Kra, R. S. and Srdoč, D., eds., Proceedings of the 13th International ${}^{14}C$ Conference. *Radiocarbon* 31 (3): 284–291.

Bard, E., Arnold, M., Fairbanks, R. G. and Hamelin, B. 1993 ${}^{230}Th\text{-}{}^{234}U$ and ${}^{14}C$ ages obtained by mass spectrometry on corals. *In* Stuiver, M., Long, A. and Kra, R. S., eds., Calibration 1993. *Radiocarbon* 35(1): 191–199.

Bard, E., Arnold, M., Hamelin, B. and Tisnerat-Iaborde, N. 1998 Radiocarbon calibration by means of mass spectrometric ${}^{230}Th/{}^{234}U$ and ${}^{14}C$ ages of corals: An updated data base including samples from Barbados, Mururoa and Tahiti. *In* Stuiver, M., ed. Calibration 1998. *Radiocarbon*, in press.

Bard, E., Arnold, M., Mangerud, J., Paterne, M., Labeyrie, L., Duprat, J., Mélières, M.-A., Sønstegaard, E. and Duplessy, J.-C. 1994 The North Atlantic atmosphere-sea surface ${}^{14}C$ gradient during the Younger Dryas climatic event. *Earth and Planetary Science Letters* 126: 275–287.

Bard, E., Hamelin, B., Fairbanks, R. G. and Zindler, A. 1990 Calibration of the ${}^{14}C$ timescale over the past 30,000 years using mass spectrometric U-Th ages from Barbados Corals. *Nature* 345: 405–410.

Bauch, D., Carstens, J. and Wefer, G. 1997 Oxygen isotope composition of living *Neogloboquadrina pachyderma* (sin.) in the Arctic Ocean. *Earth and Planetary Science Letters* 146: 47–58.

Beer, J., Johnsen, S. J., Bonani, G., Finkel, R. C., Langway, C. C., Oeschger, H., Stauffer, B., Suter, M. and Woelfli, W. 1992 ${}^{10}Be$ peaks as time markers in polar ice cores. *In* Bard, E. and Broecker, W. S., eds., *The Last Deglaciation: Absolute and Radiocarbon Chro-*

nologies. NATO ASI Series I2. Berlin, Springer Verlag: 141–153.

Berkman, P. A. and Forman, S. L. 1996 Pre-bomb radiocarbon and reservoir correction for calcareous marine species in the Southern Ocean. *Geophysical Research Letters* 23(4): 363–366.

Bond, G., Broecker, W. S., Johnsen, S. J., McManus, J., Labeyrie, L., Jouzel, J. and Bonani, G. 1993 Correlations between climate records from North Atlantic sediments and Greenland ice. *Nature* 365: 143–147.

Bond, G. C. and Lotti, R. 1995 Iceberg discharges into the North Atlantic on millennial time scales during the last Glaciation. *Science* 267: 1005–1010.

Bonhommet, N. and Babkine, J. 1967 Sur la presence d'aimantations inversées dans la chaine des Puys. *Comptes Rendues de l'Académie des Sciences* 264B: 92–94.

Broecker, W. S., Andree, M., Bonani, G., Woelfli, W., Oeschger, H., Klas, M., Mix, A. and Curry, W. 1988 Preliminary estimates for the radiocarbon age of deep water in the glacial ocean. *Paleoceanography* 3(6): 659–669.

Castagnoli, G. C., Albrecht, A., Beer, J., Bonino, G., Shen, Ch., Callegari, E., Taricco, C., Dittrich-Hannen, B., Kubik, P., Suter, M. and Zhu, G. M. 1995 Evidence for enhanced ^{10}Be deposition in Mediterranean sediments 35 kyr BP. *Geophysical Research Letters* 22(6): 707–710.

Channell, J. E. T., Hodell, D. A. and Lehman, B. 1997 Relative geomagnetic paleointensity and δ^{18}O at ODP Site 983 (Gardar Drift, North Atlantic) since 350 ka. *Earth and Planetary Science Letters* 153: 103–118.

Chappell, J. and Veeh, H. H. 1978 ^{230}Th/^{234}U age support of an interstadial sea level of –40m at 30,000 yr BP. *Nature* 276: 602–604.

Cortijo, E. (ms) 1995 La variabilité climatique rapide dans l'Atlantique Nord depuis 128 000 ans: Relations entre les calottes de glace et l'océan de surface. PhD dissertation, Université de Paris-Sud U.F.R. Scientifique D'Orsay, Paris: 235 p.

Cortijo, E., Labeyrie, L., Vidal, L., Vautravers, M., Chapman, M., Duplessy, J.-C., Elliot, M., Arnold, M., Turon, J.-L. and Auffret, G. 1997 Changes in sea surface hydrology associated with Heinrich event 4 in the North Atlantic Ocean between 40° and 60°N. *Earth and Planetary Science Letters* 146: 29–45.

Denham, C. R. and Cox, A. 1971 Evidence that the Laschamp event did not occur 13,300–30,400 years ago. *Earth and Planetary Science Letters* 13: 181–190.

Domack, E. W., Jull, A. J. T., Anderson, J. B., Linick, T. W. and Williams, C. R. 1989 Application of tandem accelerator mass-spectrometer dating to late Pleistocene-Holocene sediments of the East Antarctic continental shelf. *Quaternary Research* 31: 277–287.

Edwards, R. L., Beck, J. W., Burr, G. S., Donahue, D. J., Chapell, J. M. A., Bloom, A. L., Druffel, E. R. M. and Taylor, F. W. 1993 A large drop in atmospheric ^{14}C/^{12}C and reduced melting in the Younger Dryas, documented with ^{230}Th ages of corals. *Science* 260: 962–968.

Frank, M., Schwarz, B., Baumann, S., Kubik, P. W., Suter, M. and Mangini, A. 1997 A 200 kyr record of cosmogenic radionuclide production rate and geomagnetic field intensity from ^{10}Be in globally stacked deep-sea sediments. *Earth and Planetary Science Letters* 149: 121–129.

Fronval, T., Jansen, E., Bloemendal, J. and Johnsen, S. 1995 Oceanic evidence for coherent fluctuations in Fennoscandian and Laurentide ice sheets on millennium timescales. *Nature* 374: 443–446.

Geyh, M. A. and Schlüchter, C. 1998 Calibration of the ^{14}C time scale beyond 22,000 BP. *Radiocarbon*, this issue.

Gordon, J. E. and Harkness, D. D. 1992 Magnitude and geographic variation of the radiocarbon content in Antarctic marine life: Implications for reservoir corrections in radiocarbon dating. *Quaternary Science Reviews* 11: 697–708.

Goslar, T., Arnold, M., Bard, E., Kuc, T., Pazdur, M. F., Ralska-Jasiewiczowa, M., Rózanski, K., Tisnerat, N., Walanus, A., Wicik, B. and Wieckowski, K. 1995 High concentration of atmospheric ^{14}C during the Younger Dryas cold episode. *Nature* 377: 414–417.

Grönvold, K., Oskarsson, N., Johnsen, S. J., Clausen, H. B., Hammer, C. U., Bond, G. and Bard, E. 1995 Ash layers from Iceland in the Greenland GRIP ice core correlated with oceanic and land sediments. *Earth and Planetary Science Letters* 135: 149–155.

Grootes, P. M. and Stuiver, M. 1997 ^{18}O/^{16}O variability in Greenland snow and ice with 10^{-3} to 10^5 year time resolution. *Journal of Geophysical Research*: 102 (C12): 26,455– 26,470.

Haflidason, H., Seirup, H. P. and Kristensen, D. K. 1996 Quantification of the ^{14}C difference between terrestrial and marine environments during the Younger Dryas and the Holocene period in the North Atlantic region. *Eos Transactions AGU* 77(46), Fall Meeting Supplement: F303.

Hopkins, T. S. 1991 The GIN Seas–A synthesis of its physical oceanography and literature review 1972–1985. *Earth-Science Reviews* 30: 175–318.

Johnsen, S. J., Clausen, H. B., Dansgaard, W., Fuhrer, K., Gundestrup, N., Hammer, C. U., Iversen, P., Jouzel, J., Stauffer, B. and Steffensen, J. P. 1992 Irregular glacial interstadials recorded in a new Greenland ice core. *Nature* 359: 311–313.

Kitagawa, H. and van der Plicht, J. 1997 A 40,000-year varve chronology from Lake Suigetsu, Japan: Extension of the ^{14}C Calibration Curve. *Radiocarbon*, this issue.

Kromer, B. and Becker, B. 1993 German oak and pine ^{14}C calibration, 7200–9439 BC. *In* Stuiver, M., Long, A. and Kra, R. S., eds., Calibration 1993. *Radiocarbon* 35(1): 125–135.

Laj, C., Mazaud, A. and Duplessy, J.-C. 1996 Geomagnetic intensity and ¹⁴C abundance in the atmosphere and ocean during the past 50 kyr. *Geophysical Research Letters* 23(16): 2045–2048.

Larsen, B. 1983 Geology of the Greenland-Iceland ridge in the Denmark Strait. *In* Bott, M. H., Saxov, S., Talwani, M. and Thiede, J., eds., *Structure and Development of the Greenland-Scotland Ridge: New Methods and Concepts*. New York, Plenum Press: 425–444.

Lehman, B., Laj, C., Kissel, C., Mazaud, A., Paterne, M. and Labeyrie, L. 1996 Relative changes of the geomagnetic field intensity during the last 280 kyr from piston cores in the Azores area. *Physics of the Earth and Planetary Interiors* 93: 269–284.

Liddicoat, J. C. 1992 Mono Lake excursion in Mono Basin, California, and at Carson Sink and Pyramid Lake, Nevada. *Geophysical Journal International* 108: 442–452.

Mackensen, A., Sejrup, H. P. and Jansen, E. 1985 The distribution of living benthic foraminifera on the continental slope and rise off southwest Norway. *Marine Micropaleontology* 9: 275–306.

Malmberg, S. A. 1984 Hydrographic conditions in the East Icelandic Current and sea ice in North Icelandic waters, 1970–1980. *In* Meincke, J., Otto, L., Lee, A. J. and Dickson, R. R., eds., *Hydrobiological Variability in the North Atlantic and Adjacent Seas*. Rapports et procès-verbaux des Réunions 185. Copenhagen, Conseil international pour l'exploration de la mer: 170–178.

Malmberg, S. A. and Kristmannsson, S. S. 1992 Hydrographic conditions in Icelandic waters, 1980–1989. *In* Dickson, R. R., Mälkki, P., Radach, G., Saetre, R. and Sissenwine, M. P., eds., Hydrobiological variability in the ICES Area, 1980–1989. *ICES Marine Science Symposia* 195: 76–92.

Malmberg, S. A. and Stefansson, U. 1972 Recent changes in the water masses of the East Icelandic Current. *In* Lee, A. J. and Charnock, H., eds., *Physical Variability in the North Atlantic*. Rapports et procès-verbaux des Réunions 162. Copenhagen, Conseil international pour l'exploration de la mer:: 195–200.

McHargue, L. R., Damon, P. E. and Donahue, D. J. 1995 Enhanced cosmic-ray production of ¹⁰Be coincident with the Mono Lake and Laschamp geomagnetic excursions. *Geophysical Research Letters* 22(5): 659–662.

McIntyre, A. and Molfino, B. 1996 Forcing of Atlantic Equatorial and subpolar millennial cycles by precession. *Science* 274: 1867–1870.

Meese, D. A., Alley, R. B., Gow, A. J., Grootes, P. M., Mayewski, P. A., Ram, M., Taylor, K. C., Waddington, E. D. and Zielinski, G. A . 1994 Preliminary depth-age scale of the GISP2 ice core. *CRREL Special Report 94–1*, Cold Regions Research and Engineering Laboratory, Hanover, New Hampshire: 66 p.

Nadeau, M.-J., Schleicher, M., Grootes, P. M., Erlenkeuser, H., Gottdang, A., Mous, D. J. W., Sarnthein, J. M. and Willkomm, H. 1997 The Leibniz-Labor AMS facility at the Christian-Albrechts University, Kiel, Germany. *Nuclear Instruments and Methods in Physics Research* B123: 22–30.

Niessen, F., Grobe, H., Kipfstuhl, J. and Voelker, A. H. L. 1996 High resolution records of sediment-physical properties from the Iceland Sea: Implications for rapid oceanic variability between 10 and 85 ka. *Eos Transactions AGU* 77(46), Fall Meeting Supplement: F24.

Olafsdóttir, Th. 1975 Jökulgardur a sjavarbotni ut af Breidafirdi (A moraine ridge on the Iceland shelf west of Breidafjördur). *Natturufraedingurinn* 45: 31–36.

Plummer, M. A., Phillips, F. M., Fabryka-Martin, J., Turin, H. J., Wigand, P. E. and Sharma, P. 1997 Chlorine-36 in fossil rat urine: An archive of cosmogenic nuclide deposition during the past 40,000 years. *Science* 277: 538–541.

Raisbeck, G. M., Yiou, F., Bourles, D., Lorius, C., Jouzel, J. and Barkov, N. I. 1987 Evidence for two intervals of enhanced ¹⁰Be deposition in Antarctic ice during the last glacial period. *Nature* 326: 273–277.

Rasmussen, T. L., Thomsen, E., Labeyrie, L. and van Weering, T. C. E. 1996a Circulation changes in the Faeroe-Shetland Channel correlating with cold events during the last glacial period (58–10 ka). *Geology* 24(10): 937–940.

Rasmussen, T. L., Thomsen, E., van Weering, T. C. E. and Labeyrie, L. 1996b Rapid changes in surface and deep water conditions at the Faeroe margin during the last 58,000 years. *Paleoceanography* 11(6): 757–771.

Robinson, C., Raisbeck, G. M., Yiou, F., Lehman, B. and Laj, C. 1995 The relationship between ¹⁰Be and geomagnetic field strength records in central North Atlantic sediments during the last 80 ka. *Earth and Planetary Science Letters* 136: 551–557.

Ruddiman, W. F. 1977 Late Quaternary deposition of ice-rafted sand in the subpolar North Atlantic (lat. 40° to 65°N). *Geological Society of America Bulletin* 88: 1813–1827.

Samtleben, C., Schäfer, P., Andruleit, H., Baumann, A., Baumann, K.-H., Kohly, A., Matthiessen, J., Schröder-Ritzrau, A. and Synpal Working Group 1995 Plankton in the Norwegian-Greenland Sea: From living communities to sediment assemblages - an actualistic approach. *Geologische Rundschau* 84: 108–136.

Sarnthein, M., Jansen, E., Weinelt, M., Arnold, M., Duplessy, J.-C., Erlenkeuser, H., Flatoy, A., Johannessen, G., Johannessen, T., Jung, S., Koc, N., Labeyrie, L., Maslin, M., Pflaumann, U. and Schulz, H. 1995 Variations in Atlantic surface ocean paleoceanography, 50–80°N: A time-slice record of the last 30,000 years. *Paleoceanography* 10(6): 1063–1094.

Schleicher, M., Grootes, P. M., Nadeau, M.-J. and Schoon, A. 1998 The carbonate ¹⁴C background and its components at the Leibniz AMS facility. *Radiocarbon*, this issue.

Schramm, A., Stein, M. and Goldstein, S. L. 1996 U-series and ¹⁴C dating of Lake Lisan (Paleo- Dead Sea) sediments: Implications for ¹⁴C time scale calibration and relation to global paleoclimate. *Eos Transactions AGU* 77(46), Fall Meeting Supplement: F303.

____ 1997 U-series and ¹⁴C dating of Lake Lisan (Paleo- Dead Sea) sediments and absolute calibration of the ¹⁴C time scale. *Terra Nova* 9, Abstract supplement no. 1: 629.

Seidov, D., Sarnthein, M., Stattegger, K., Prien, R. and Weinelt, M. 1996 North Atlantic ocean circulation during the last glacial maximum and subsequent meltwater event: A numerical model. *Journal of Geophysical Research* 101(C7): 16,305–16,332.

Simstich, J., Sarnthein, M., Erlenkeuser, H. and Schiebel. R. (ms) Differential calcification habitats of planktonic foraminifers in the Nordic Seas: δ¹⁸O records of the thermocline. In preparation.

Stefansson, U. 1962 North Icelandic Waters. *Rit Fiskideildar* 3: 269 p.

Stocker, T. F. and Wright, D. G. 1998 The Effect of a succession of ocean ventilation changes on ¹⁴C. *Radiocarbon*, this issue.

Stuiver, M. and Braziunas, T. F. 1993 Modeling atmospheric ¹⁴C influences and ¹⁴C ages of marine samples to 10,000 BC. *In* Stuiver, M., Long, A. and Kra, R. S., eds., Calibration 1993. *Radiocarbon* 35(1): 137–189.

Stuiver, M. and Reimer, P. J. 1993 Extended ¹⁴C data base and revised CALIB 3.0 ¹⁴C age calibration program. *In* Stuiver, M., Long, A. and Kra, R. S., eds., Calibration 1993. *Radiocarbon* 35(1): 215–230.

Swift, J. H. and Aagaard, K. 1981 Seasonal transitions and water mass formation in the Iceland and Greenland seas. *Deep-Sea Research* 28A(10): 1107–1129.

Trauth, M. H., Sarnthein, M. and Arnold, M. 1997 Bioturbational mixing depth and carbon flux at the seafloor. *Paleoceanography* 12(3): 517–526.

Vinje, T. E. 1977 Sea ice conditions in the European sector of the marginal seas of the Arctic, 1966–1975. *Norsk Polarinstitutt Årbok*: 163–174.

Vlag, P., Thouveny, N., Wiliamson, D., Rochette, P. and Ben-Atig, F. 1996 Evidence for a geomagnetic excursion recorded in the sediments of Lac St. Front, France: A link with the Laschamp excursion? *Journal of Geophysical Research* 101(B12): 28,211–28,230.

Voelker, A. H. L., Sarnthein, M. and Erlenkeuser, H. 1996 80 000 years of millennial climate oscillations off Northern Iceland and the history of water mass exchange across the Denmark Strait. *Eos Transactions AGU* 77(17), Spring Meeting Supplement: S165.

Voelker, A. H. L., Sarnthein, M., Erlenkeuser, H., Grootes, P. and Nadeau, M.-J. 1997 Meltwater spikes in the Nordic Seas: Are they triggering the Dansgaard-Oeschger climate oscillations? *Terra Nova* 9, Abstract supplement no. 1: 209.

Vogel, J. C. 1983 ¹⁴C variations during the Upper Pleistocene. *In* Stuiver, M. and Kra, R., eds., Proceedings of the 11th International ¹⁴C Conference. *Radiocarbon* 25(2): 213–218.

Vogel, J. C. and Kronfeld, J. 1997 Calibration of radiocarbon dates for the late Pleistocene using U/Th dates on stalagmites. *Radiocarbon* 39(1): 27–32.

Vogt, P. R., Johnson, G. L. and Kristjansson, L. 1980 Morphology and magnetic anomalies north of Iceland. *In* Jacoby, W., Björnsson, A. and Möller, D., eds., Iceland: Evolution, active tectonics, and structure. *Journal of Geophysics* 47: 67–80.

Weeks, R., Laj, C., Endignoux, L., Fuller, M., Roberts, A., Manganne, R., Blanchard, E. and Goree, W. 1993 Improvements in long-core measurement techniques: Applications in palaeomagnetism and palaeoceanography. *Geophysical Journal International* 114: 651–662.

Weinelt, M., Sarnthein, M., Pflaumann, U., Schulz, H., Jung, S. and Erlenkeuser, H. 1996 Ice-free Nordic Seas during the last glacial maximum? Potential sites of deepwater formation. *Palaeoclimates* 1: 283–309.

Wilson, A. T. 1995 Application of AMS ¹⁴C dating to ice core research. *In* Cook, G. T., Harkness, D. D., Miller, B. F. and Scott, E. M., eds., Proceedings of the 15th International ¹⁴C Conference. *Radiocarbon* 37(2): 637–641.

Wu, G. and Hillaire-Marcel, C. 1994 Accelerator mass spectrometry radiocarbon stratigraphies in deep Labrador Sea cores: Paleoceanographic implications. *Canadian Journal of Earth Sciences* 31: 28–47.

Yiou, F., Raisbeck, G. M., Baumgartner, S., Beer, J., Hammer, C., Johnsen, S., Jouzel, J., Kubik, P. W., Lestringuez, J., Stievenard, M., Suter, M. and Yiou, P. 1997 Beryllium 10 in the Greenland Ice Core Project ice core at Summit, Greenland. *Journal of Geophysical Research*: 102 (C12): 26,783–26,794.

Zielinski, G. A., Mayewski, P. A., Meeker, L. D., Whitlow, S. and Twickler, M. S. 1996 A 110,000 year record of explosive volcanism from the GISP2 (Greenland) ice core. *Quaternary Research* 45: 109–118.

APPENDIX: TABLES 1A AND 1B

TABLE 1A. AMS ^{14}C Measurements on Planktic (p) and Benthic (b) Foraminifera in Core PS2644

Lab code	Composite depth (m)	AMS ^{14}C age ± 1σ (yr) ($T_{1/2}$ = 5568 yr)	Cal. age in GISP2 (yr)	Age shift (yr) (cal. − ^{14}C age)
KIA1557	0.005(p)	−580 ± 30		
KIA733	0.005(p)	−630 ± 20		
KIA3348	0.18(p)	5360 ± 40		
KIA734	0.21(p)	10,190 ± 110		
KIA74	0.22(p)	9580 ± 60	11,380	1800
KIA757	0.24(p)	6820 ± 40		
KIA3344	0.24(p)	10,460 ± 60		
KIA3345	0.35(p)	3800 ± 30		
KIA801	0.36(p)	4330 ± 30		
KIA735	0.50(p)	12,050 ± 60	14,500	2450
KIA3346	0.55(p)	8610 ± 50		
KIA802	0.65(p)	13,970 ± 60	15,650	1680
KIA741	0.65(b)	13,650 ± 90	15,650	2000
KIA77	0.71(p)	14,680 ± 210	16,050	1370
KIA1649	0.71(b)	14,050 ± 80	16,050	2000
KIA736	0.80(p)	14,490 ± 80	17,220	2730
KIA742	0.80(b)	13,730 ± 90	17,220	3490
KIA743	0.80(b)	14,090 ± 90	17,220	3130
KIA78	0.86(p)	14,810 ± 240	17,420	2610
KIA1650	0.86(b)	14,320 +90/−80	17,420	3100
KIA79	0.91(p)	15,260 +220/−210	17,660	2400
KIA737	0.95(p)	14,980 ± 80	17,990	3010
KIA744	0.95(b)	14,750 ± 90	17,990	3240
KIA803	1.05(p)	16,110 ± 70	18,100	1990
KIA804	1.13(p)	17,230 ± 90	18,840	1610
KIA1641	1.13(b)	15,390 ± 120	18,840	3450
KIA805	1.21(p)	18,560 ± 100		
KIA80	1.26(p)	19,330 +340/−330		
KIA806	1.29(p)	18,900 ± 90	21,640	2740
KIA745	1.29(b)	17,340 ± 160	21,640	4300
KIA1647	1.33(p)	20,700 ± 160		
KIA746	1.33(b)	21,030 ± 200		
	1.34(p)	21,010 (interpolated)	24,100	3090
	1.34(b)	21,050 (interpolated)	24,100	3050
KIA710	1.37(p)	21,940 ± 180		
KIA747	1.37(b)	21,390 +200/−190		
KIA738	1.43(p)	22,380 ± 180	25,700	3320
KIA807	1.49(p)	23,910 +170/−160		
KIA739	1.63(p)	25,300 +300/−290	28,990	3690
KIA1642	1.63(b)	23,380 +220/−210	28,990	
KIA81	1.76(p)	27,150 +910/−820	30,100	2950
KIA740	1.80(p)	27,040 +300/−290	30,300	3260
KIA758	1.99(p)	27,630 +340/−320	30,380	3750
KIA82	2.06(p)	28,940 +1150/−1010	31,770	2830
KIA808	2.18(p)	28,070 ± 200	32,180	4110
KIA809	2.29(p)	29,000 ± 210	32,780	3780
KIA759	2.36(p)	29,790 +440/−410	33,170	3380
KIA810	2.41(p)	28,730 +230/−220	33,280	4550
KIA1648	2.51(p)	28,650 +420/−400	33,490	4840
KIA1643	2.52(b)	25,200 +420/−400	33,520	
KIA760	2.53(p)	29,740 +270/−260	33,610	3870
KIA811	2.60(p)	29,710 +260/−250	33,880	4170

TABLE 1A. AMS [14]C Measurements on Planktic (p) and Benthic (b) Foraminifera in Core
PS2644 *(Continued)*

Lab code	Composite depth (m)	AMS ^{14}C age ± 1σ (yr) ($T_{1/2}$ = 5568 yr)	Cal. age in GISP2 (yr)	Age shift (yr) (cal. – [14]C age)
KIA812	2.70(p)	30,640 +260/–250	34,300	3660
KIA761	2.75(p)	31,180 +500/–470	34,520	3340
KIA813	2.83(p)	31,400 +270/–260	34,700	3300
KIA814	2.92(p)	31,550 +280/–270	35,140	3590
KIA75	2.975(p)	31,680 +1670/–1380	35,310	3630
KIA815	3.04(p)	31,530 +280/–270	35,580	4050
KIA816	3.12(p)	32,150 +290/–280	35,770	3620
KIA817	3.20(p)	32,010 +330/–310	36,230	4220
KIA818	3.25(p)	32,740 +330/–320	36,330	3590
KIA819	3.31(p)	32,760 +360/–340	36,820	4060
KIA820	3.40(p)	33,030 +320/–310	37,410	4380
KIA821	3.44(p)	33,520 +350/–330	37,630	4110
KIA1449	3.59(p)	32,260 +560/–520	38,300	6040
KIA889	3.67(p)	34,450 +930/–840	38,570	4120
KIA890	3.79(p)	34,750 +990/–880	39,850	5100
KIA1552	3.89(p)	32,960 +600/–560	40,420	7460
KIA910	3.90(p)	32,850 +770/–710	40,470	7620
KIA3347	4.05(p)	36,410 +1160/–1020	40,820	4410
KIA911	4.14(p)	37,050 +1400/–1190	41,090	4040
KIA1644	4.14(b)	37,340 +1190/–1040	41,090	3750
KIA891	4.22(p)	38,590 +1640/–1360	41,550	2960
KIA912	4.35(p)	38,810 +1670/–1380	41,800	2990
KIA913	4.60(p)	39,310 +1820/–1480	42,530	3220
KIA914	4.74(p)	42,130 +2690/–2010	43,260	1130
KIA1553	4.82(p)	43,740 +2540/–1930	43,890	150
KIA1554	4.88‡(p)	45,010 +3070/–2220		
KIA3975	4.88§(p)	41,770 +880/–790		
	4.88(p) *average*	*42,300 +840/–760*	44,210	1910
KIA892	4.92(p)	44,070 +3580/–2470		
KIA3976	4.92§(p)	42,070 +920/–830		
	4.92(p) *average*	*42,300 +880/–800*	44,390	2090
KIA1555	5.03(p)	45,650 +3470/–2420		
KIA4120	5.03§(p)	43,330 +1150/–1010		
	5.03(p) *average*	*43,750 +1080/–950*	44,720	970
Gif 97134	5.07*‡(p)	41,010 ± 690		
KIA1556	5.07(p)	44,470 +2860/–2100		
KIA4121	5.07§(p)	43,340 +1080/–950		
	5.07(p) *average*	*43,540 +990/–880*	44,850	1310
KIA915	5.30(p)	42,470 +2810/–2080		
KIA4151	5.30§(p)	44,750 +1360/–1160		
	5.30(p) *average*	*44,390 +1200/–1040*	45,360	970
KIA4122	5.35§(p)	44,050 +1180/–1030	45,940	1890
KIA893	5.42‡(p)	43,540 +3300/–2330		
Gif 97136	5.42*‡(p)	43,530 ± 890		
KIA3506	5.42§(p)	45,500 +810/–730		
KIA3696	5.42§(p)	45,190 +1200/–1040		
	5.42(p) *average*	*45,410 +660/–610*	46,530	1120
KIA3507	5.49§(p)	45,090 +780/–710		
KIA3697	5.49§(p)	45,170 +1240/–1070		
	5.49(p) *average*	*45,120 +650/–600*	47,030	1910
KIA3508	5.64§(p)	41,210 +480/–460		
KIA3698	5.64§(p)	43,210 +990/–880		
	5.64(p) *average*	*41,750 +430/–410*		
KIA3770	5.65§(p)	47,000 +1600/–1330		

TABLE 1A. AMS ^{14}C Measurements on Planktic (p) and Benthic (b) Foraminifera in Core PS2644 *(Continued)*

Lab code	Composite depth (m)	AMS ^{14}C age ± 1σ (yr) ($T_{1/2}$ = 5568 yr)	Cal. age in GISP2 (yr)	Age shift (yr) (cal. – ^{14}C age)
KIA4123	5.65§(p)	43,880 +1260/–1090		
	5.65(p) *average*	*45,560 +990/–880*		
KIA3771	5.68§(p)	50,720 +2510/–1910		
KIA4124	5.68§(p)	46,070 +1550/–1300		
	5.68(p) *average*	*48,420 +1330/–1140*		
KIA3509	5.80§(p)	47,410 +1090/–960		
KIA3699	5.80§(p)	49,470 +2120/–1680		
	5.80(p) *average*	*48,040 +960/–860*	49,190	1150
KIA3768	5.85§(p)	48,620 +1870/–1520		
KIA3510	5.90§(p)	47,490 +1060/–930		
KIA3700	5.90§(p)	48,100 +1810/–1480		
	5.90(p) *average*	*47,670 +890/–800*		
KIA3769	5.98§ p)	50,890 +2610/–1970		
KIA3511	6.00§‡(p)	43,700 +670/–620		
KIA3701	6.00§(p)	50,420 +2490/–1900		
KIA3977	6.00§(p)	46,880 +1720/–1410		
	5.98–6.00(p) *average*	*49,400 +1210/–1050*		
KIA3762	6.05§(p)	51,500 +2930/–2140		
KIA3762	6.05§(p)	50,110 +2340/–1810		
	6.05(p) *average*	*50,770 +1750/–1440*		
KIA3512	6.10§ p)	50,480 +1500/–1260		
KIA3702	6.10§(p)	51,550 +2830/–2090		
	6.10(p) *average*	*50,780 +1280/–1110*		
KIA3763	6.27§(p)	50,080 +2370/–1830		
KIA3763	6.27§(p)	50,710 +2720/–2030		
	6.27(p) *average*	*50,380 +1700/–1400*		
KIA3761	6.57§(p)	52,810 +3480/–2420		
KIA3761	6.57§(p)	53,240 +3640/–2500		
KIA3979	6.57§(p)	49,370 +2470/–1890		
	6.57(p) *average*	*51,870 +1670/–1380*	53,260	1390
KIA3978	6.57§(b)	45,110 +1360/–1170		
KIA3764	6.65§(p)	52,770 +3700/–2520		
KIA3764	6.65§(p)	52,070 +3200/–2280		
KIA3980	6.65§(p)	47,750 +1950/–1570		
	6.65(p) *average*	*50,760 +1480/–1250*	53,260	2500
KIA4125	6.75§(p)	50,030 +2680/–2010		
KIA176	8.25(p)	34,930 (34,680–37,870)		apparent back-ground ages (range)
KIA711	8.25(p)	42,060 (40,520–43,790)		
KIA828	8.85(p)	44,750 (42,960–47,150)		
KIA828	8.85(p)	46,340 (45,980–47,540)		
GifA97137	8.85*(p)	53,150 ± 890		
KIA3513	8.85§ (p)	56,540 (54,880–59,080)		
KIA3513	8.85§(p)	57,530 (56,410–60,990)		
KIA3703	8.85§(p)	51,140 (49,260–53,350)		
KIA3703	8.85§(p)	55,770 (54,550–59,340)		
KIA3981	8.85§(p)	50,590 (47,990–55,030)		
KIA3981	8.85§(p)	53,610 (50,220–59,020)		

Notes: Ages (except for backgrounds) are corrected for a global-average ocean reservoir effect by –400 yr. Calendar ages are obtained by correlation of δ^{18}O minima spikes in core PS2644 with annual-layer dated δ^{18}O minima spikes in the GISP2 ice core (Meese *et al.* 1994). The composite depth is based on a core fit between the giant box core and the gravity-core records, the original core depths of which are increased by 0.06 m.

*= ^{14}C dates measured in Gif-sur-Yvette, France; † = outlier dates ignored in Fig. 6 (see text); ‡ = samples which we rank at low weight and do not include into the calculation of weighted-average values; § = samples treated with peroxide and attached "wet" to the carbonate preparation line (Schleicher *et al.* 1998).

TABLE 1B. AMS ^{14}C Measurements on Planktic (p) Foraminifera in Core 23071

Lab code	Composite depth (m)	AMS ^{14}C age ± 1σ (yr) ($T_{1/2}$ = 5568 yr)	Cal. age in GISP2 (yr)	Age shift (yr) (cal. − ^{14}C age)
AAR1354	0.0075#(p)	1610 ± 70		
GifA	0.15*(p)	6680 ± 120		
KIA829	0.20(p)	7560 ± 60		
KIA706	0.255(p)	5440 ± 50		
KIA830	0.435(p)	10,570 ± 70		
KIA831	0.645(p)	11,760 ± 100		
GifA	0.75*(p)	12,550 ± 220		
GifA	0.82*(p)	13,600 ± 300		
KIA426	0.835(p)	13,835 ± 100		
GifA	0.93*(p)	14,790 ± 190		
KIA832	0.955(p)	17,030 ± 120		
KIA707	0.99(p)	16,580 ± 130		
GifA	1.12*(p)	16,550 ± 200		
GifA	1.16*(p)	16,690 ± 230		
GifA	1.20*(p)	16,990 ± 220		
GifA	1.40*(p)	18,520 ± 240		
GifA	1.50*(p)	18,790 ± 240		
GifA	1.70*(p)	21,430 ± 300		
GifA	2.10*(p)	23,730 ± 360		
KIA833	2.40(p)	25,730 +330/−310	28,990	3260
KIA427	2.54(p)	26,350 +340/−330	30,300	3950
GifA	2.73*(p)	28,020 ± 560	32,180	4160
KIA708	3.09(p)	31,630 +740/−680		
KIA709	3.27(p)	32,890 +870/−780	38,570	5680
GifA	3.33*(p)	39,600 ± 1800		
KIA834	3.38(p)	37,720 +1320/−1540		
KIA3514	3.45§(p)	37,110 +320/−310		
KIA894	3.58(p)	41,200 +1910/−1540		
KIA895	3.76(p)	45,180 +3400/−2380		
KIA3766	3.76§(p)	45,000 +1160/−1010		
	3.76(p) *average*	45,030 +1080/−950		
KIA3765	3.89§(p)	45,870 +1290/−1110		
KIA896	4.01(p)	> 42,970		
KIA3515	4.02§(p)	44,510 +700/−650		
KIA3767	4.06§(p)	48,850 +1980/−1590		
KIA897	4.17(p)	>45,520		
KIA3516	4.17§(p)	50,110 +1500/−1260		
KIA898	4.26(p)	>46,180		
KIA3517	4.26§(p)	53,610 +2290/−1780		
KIA836	5.34(p)	45,450 (44,100–47,740)		apparent back-
KIA3518	5.34§(p)	56,470 (54,050–57,910)		ground ages
KIA3518	5.34§(p)	57,690 (56,820–61,910)		(range)
KIA3704	5.34§(p)	52,910 (52,630–56,030)		

Notes: Ages (except for backgrounds) are corrected for a global-average ocean reservoir effect by −400 yr. Calendar ages are obtained by correlation of δ^{18}O minima spikes in core 23071 with annual-layer dated δ^{18}O minima spikes in the GISP2 ice core (Meese *et al.* 1994). The composite depth is based on a core fit between the giant box core and the kastencore records, the original core depths of which were reduced by 0.10 m.

* and §, see Table 1A (ages measured in Gif-sur-Yvette, from Sarnthein *et al.* 1995); # = date measured in Aarhus (Samtleben *et al.* 1995).